



## Coupling between minimum scattering antennas

Andersen, J.; Lessow, H; Schjær-Jacobsen, Hans

*Published in:*

I E E E Transactions on Antennas and Propagation

*Link to article, DOI:*

[10.1109/TAP.1974.1140912](https://doi.org/10.1109/TAP.1974.1140912)

*Publication date:*

1974

*Document Version*

Publisher's PDF, also known as Version of record

[Link back to DTU Orbit](#)

*Citation (APA):*

Andersen, J., Lessow, H., & Schjær-Jacobsen, H. (1974). Coupling between minimum scattering antennas. *I E E E Transactions on Antennas and Propagation*, 22(6), 832-835. <https://doi.org/10.1109/TAP.1974.1140912>

---

### General rights

Copyright and moral rights for the publications made accessible in the public portal are retained by the authors and/or other copyright owners and it is a condition of accessing publications that users recognise and abide by the legal requirements associated with these rights.

- Users may download and print one copy of any publication from the public portal for the purpose of private study or research.
- You may not further distribute the material or use it for any profit-making activity or commercial gain
- You may freely distribute the URL identifying the publication in the public portal

If you believe that this document breaches copyright please contact us providing details, and we will remove access to the work immediately and investigate your claim.

## Coupling Between Minimum Scattering Antennas

J. BACH ANDERSEN, H. A. LESSOW, AND  
H. SCHJÆR-JACOBSEN

**Abstract**—Coupling between minimum scattering antennas (MSA's) is investigated by the coupling theory developed by Wasyliwskyj and Kahn. Only rotationally symmetric power patterns are considered, and graphs of relative mutual impedance are presented as a function of distance and pattern parameters. Crossed-dipoles and helices are considered in order to establish a correspondence with simple antenna structures.

## INTRODUCTION

In many applications, e.g., phased arrays and multibeam antennas, the interaction between antenna elements is often important in the evaluation of the total antenna system performance. This communication is concerned with an idealized class of elements consisting of minimum scattering antennas (MSA's) [1]. Works have been published, notably by Wasyliwskyj and Kahn [2], [3], on coupling theory for MSA's. The power of the technique is that the complex relative mutual impedance is completely given by the power pattern of a single element, where the mutual impedance is taken relative to the real part of the self-impedance of one element. The MSA concept is used here to compute the relative mutual impedance between two elements for various spacings between the elements and for various power patterns. Once the relative mutual impedance is known it is a simple matter to find coupling loss, scattered patterns, etc.

The practical usefulness of the MSA concept depends on the extent to which coupling among realistic antennas is adequately covered by the theory. Therefore another purpose of this communication is to investigate two commonly used element types, namely crossed-dipoles and helices, and compare coupling data obtained by the MSA approach with other calculations and experimental data.

## MUTUAL IMPEDANCE THEORY

Consider two identical reciprocal MSA's I and II situated along the  $z'$  axis in Fig. 1. From Wasyliwskyj and Kahn [2, eqs. (71b) and (72)] we find for the normalized mutual impedance

$$Z_{12} = 2 \int_0^{2\pi} d\phi' \int_{\Gamma} \sin \alpha d\alpha \exp(-j\mathbf{k} \cdot \mathbf{d}) P(\alpha, \phi') \quad (1)$$

where  $P(\alpha, \phi')$  is the power pattern for one antenna.  $P(\alpha, \phi')$  is normalized such that the total radiated power is unity. This means that the real part of the self-impedance of one element is equal to unity.  $\alpha$  and  $\phi'$  are spherical coordinates and the  $\alpha$  integration is to be taken in the complex  $\alpha$  plane, with  $0 \leq \alpha \leq \pi/2$  along the real  $\alpha$  axis and  $0 \leq \text{Im}(\alpha) < j\infty$  along the line  $\text{Re}(\alpha) = \pi/2$ .  $\mathbf{d} = d\hat{z}'$  is a vector with direction from antenna I to antenna II and its length equals the distance between the two antennas.  $\mathbf{k}$  is the propagation vector.

To simplify things we consider only power patterns with rotational symmetry, the axis of symmetry being the  $y'$  axis. Thus we assume that  $P(\alpha, \phi')$  is a function of  $\theta$  only,  $\theta$  being measured from the  $y'$  axis. The pattern function is expanded in a power series in  $\cos \theta$ , each term in the series contributing both to the real and imaginary part of the mutual impedance. Restricting ourselves to two terms, we find

$$P(\theta) = 1 + A \cos^N(\theta), \quad 0 \leq \theta \leq \frac{\pi}{2} \quad (2)$$

## REFERENCES

- [1] E. K. Damon, "The near fields of long end-fire dipole arrays," *IRE Trans. Antennas Propagat.*, vol. AP-10, pp. 511-523, Sept. 1962.
- [2] E. G. Neumann, "Radiation mechanism of dielectric rod and Yagi aerials," *Electron. Lett.*, vol. 6, p. 528, 1970.
- [3] H. W. Ehrenspeck and H. Poehler, "A new method for obtaining maximum gain from Yagi antennas," *IRE Trans. Antennas Propagat.*, vol. AP-7, pp. 379-386, Oct. 1959.
- [4] W. W. Hansen and J. R. Woodyard, "A new principle in directional antenna design," *Proc. IRE*, vol. 26, pp. 333-345, Mar. 1938.
- [5] S. Silver, *Microwave Antenna Theory and Design*. New York: McGraw-Hill, 1949.

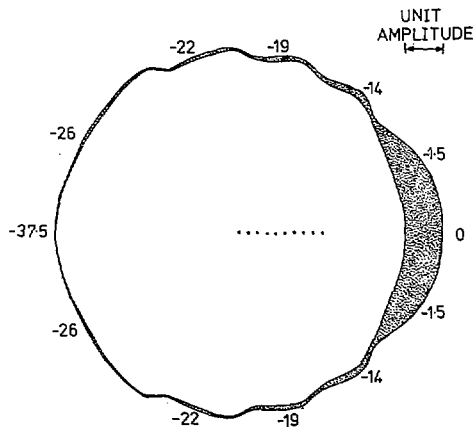


Fig. 4. Near-field amplitude distribution around ordinary endfire array.

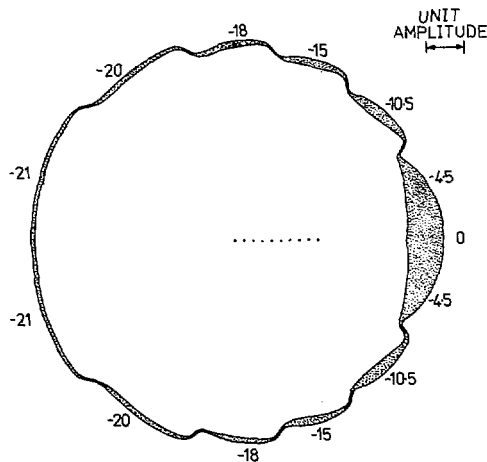


Fig. 5. Near-field amplitude distribution from Hansen-Woodyard array.

relatively flat regions beyond the ripples on the wavefronts can be seen to correspond with sidelobes.

Figs. 4 and 5 illustrate the near-field amplitude distributions along the wavefronts for the two types of array, and these diagrams were made in the following way. The amplitudes were computed for points on the fourth wavefronts on Figs. 1 and 2. The amplitudes are represented by proportional length lines drawn orthogonal to, and with their centers at, the wavefronts. Joining the inner and outer line extremities gave the forms shown. These then are wavefront diagrams where the thickness of the figure represents the relative electric field amplitude. The relative amplitudes at certain points are also given in numbers although these, unlike the figure thicknesses, are expressed in decibels. As would be expected, the near-field amplitudes are highest at the angular positions corresponding to the main and sidelobe maxima. This is particularly evident in the Hansen-Woodyard case.

Manuscript received March 27, 1974; revised May 30, 1974. This work was supported by ESRO under ESTEC Contract 1698/72AA. J. Bach Andersen is with the Danish Engineering Academy, Aalborg, Denmark. H. A. Lessow and H. Schjær-Jacobsen are with the Electromagnetics Institute, Technical University of Denmark, Lyngby, Denmark.

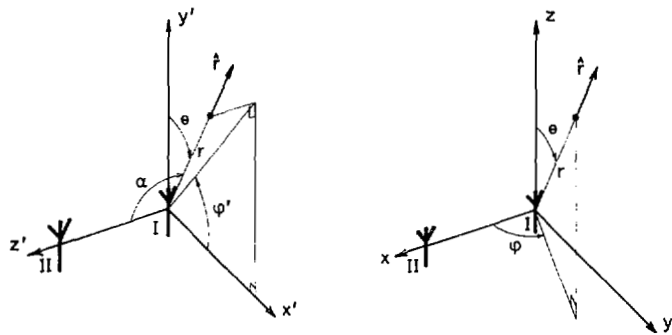


Fig. 1. Coordinate systems \$(r, \alpha, \phi')\$ and \$(r, \theta, \phi)\$.

where \$A\$ is a real number larger than \$-1\$. The two parameters \$N\$ and \$A\$ determine the beamwidth and the sidelobe, respectively. For easy reference, examples of the patterns are shown in Fig. 2 for \$A = 1\$ and \$A = 1000\$; note the different scale in the two cases.

Using (2) in (1) we find after simple manipulations [4]

$$Z_{12} = \left\{ j \frac{\exp(-jkd)}{kd} + \frac{A}{\pi^{1/2}} \frac{\Gamma((N+1)/2)}{\Gamma((N/2)+1)} \cdot (Z_1 + jZ_2) \right\} / \left( 1 + \frac{A}{(N+1)} \right) \quad (3)$$

where

$$Z_1 = \int_0^1 \exp(-jkt) [(1-t^2)^{1/2}]^N dt \quad (4)$$

and

$$Z_2 = \int_0^\infty \exp(-kt) [(1+t^2)^{1/2}]^N dt. \quad (5)$$

In the examples to follow, \$Z\_1\$ and \$Z\_2\$ are evaluated numerically. \$\Gamma(x)\$ is the gamma function with argument \$x\$.

NUMERICAL RESULTS

In this section we consider only the absolute value of \$Z\_{12}\$, since this will be the determining factor for the relative strength of a parasitically excited neighbor antenna. In Fig. 3 the absolute value of the normalized mutual impedance \$Z\_{12}\$ is shown as a function of \$N\$ and \$A\$ for a spacing \$d = 0.4\lambda\$. For this small spacing, small values of \$A\$ and large values of \$N\$ have to be chosen in order to minimize the mutual interaction. The minimum value of \$|Z\_{12}|\$ may be evaluated from (3) under the assumption that \$N\$ is large. \$Z\_1\$ may be neglected in comparison with \$Z\_2\$, which, with a proper \$A\$, cancels the imaginary part of the first term leaving only the real part, i.e.,

$$|Z_{12}|_{\min} = \frac{|\sin kd|}{kd}. \quad (6)$$

For \$d = 0.4\lambda\$ this equals 0.234 and is obtained for very small values of \$A\$. This optimum is mostly of academic interest, since \$|Z\_{12}|\$ will be rather sensitive to \$A\$, and it is difficult to see how the antenna should be realized. Equation (6) is only an approximation. The true minimum must be found numerically and is indicated as a broken line in Figs. 4(a) and (b). The results show a very good agreement with (6) for \$d < 0.5\lambda\$ while the minimum is essentially zero for \$d > 0.5\lambda\$, an important result.

Fig. 4 shows numerical results for \$A = 1\$ and \$A = 1000\$ as a function of \$d/\lambda\$ and \$N\$. The curves are self-explanatory. Note that the small values of \$N\$ are favored for \$d/\lambda\$ small, which may be interpreted in the following way. For small spacings the reactive near-

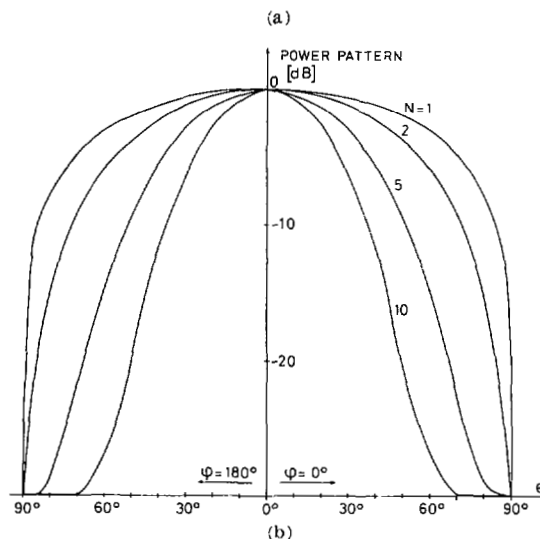
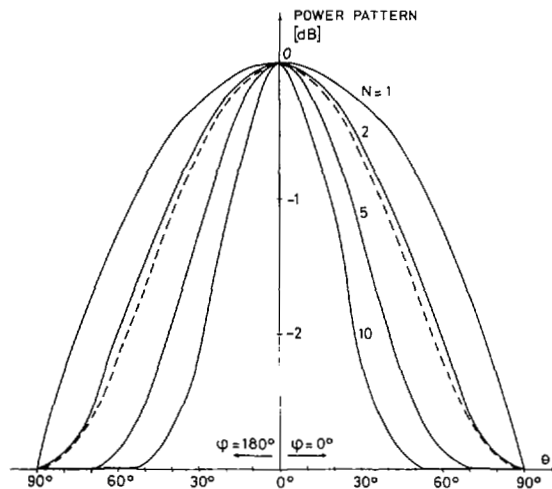


Fig. 2. (a) Power pattern for one MSA. \$P(\theta) = 1 + \cos^N \theta\$. Dashed curve shows pattern of crossed-dipole in plane bisecting arms. (b) Power pattern for one MSA. \$P(\theta) = 1 + 1000 \cos^N \theta\$.

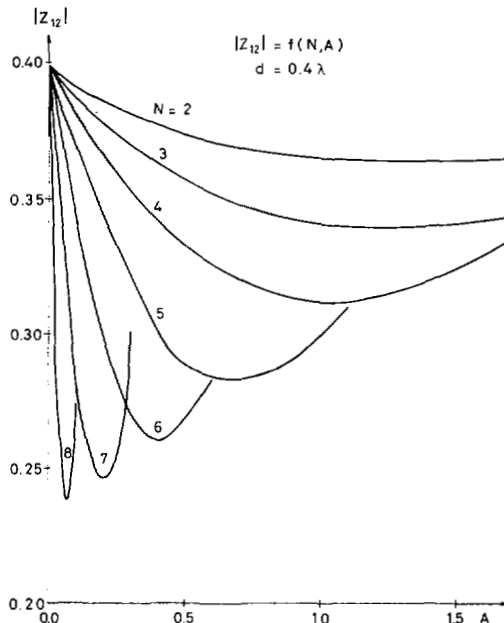


Fig. 3. Absolute value of relative mutual impedance between two MSA's.

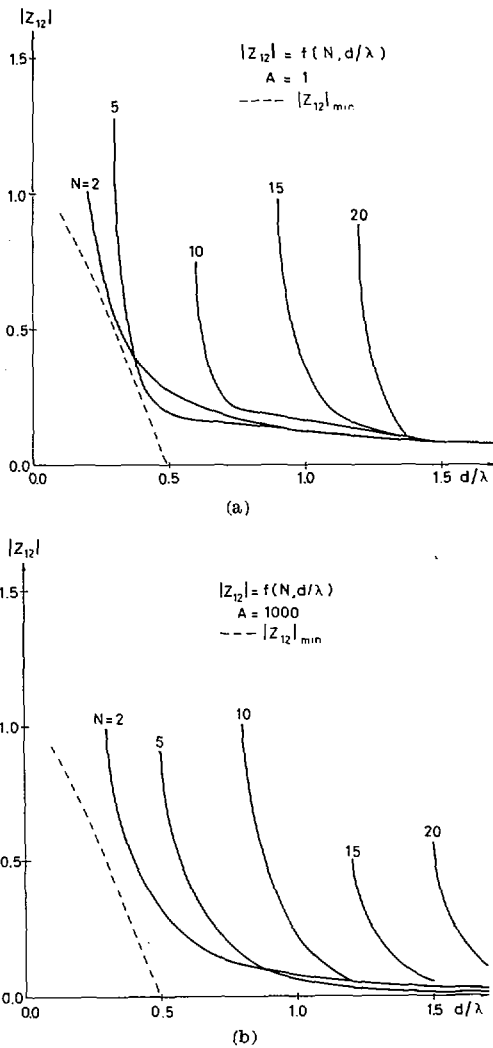


Fig. 4. Absolute value of relative mutual impedance between two MSA's.

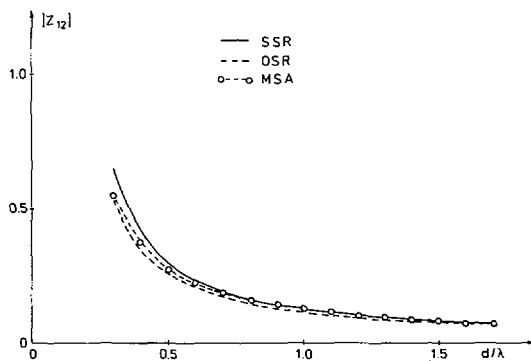


Fig. 5. Absolute value of relative mutual impedance between two antennas. Crossed-dipoles with minimum coupling with same sense of rotation (SSR) and opposite sense of rotation (OSR). Minimum scattering antennas (MSA).

fields are interacting; in order to minimize their magnitude, a broad pattern is required. This is of course well known, but here we have a quantitative measure of the interaction.

It may also be noted that for  $d/\lambda$  large,  $A = 1000$  gives less coupling than  $A = 1$ . This is also natural since for far-field conditions the pattern with a null ( $-30$  dB) in the direction between the two antennas will give the smallest coupling. For small spacings the opposite is true.

The applicability of the curves may best be shown by an example. A multibeam reflector antenna is fed by feed antennas with patterns that may be approximated by  $A = 1000, N = 5$ . A spacing larger than  $0.9\lambda$  is required in order that  $|Z_{12}| < 0.1$ , which in most cases will be sufficient.

### COMPARISONS WITH REALISTIC ANTENNAS

In order to investigate the validity of the previous calculations, comparisons have been made with realistic antenna types.

#### Crossed-Dipoles

A crossed-dipole-antenna with feeding network is not an MSA [5] and does not have a rotationally symmetric pattern. Nevertheless it is interesting to make a comparison.

The power pattern of one crossed-dipole may be approximated with  $A = 1$  and  $N = 2$  in (2); see Fig. 2(a). The resulting normalized mutual impedance is shown in Fig. 5 as a function of spacing. Also shown are the calculations of mutual impedance between actual coplanar crossed-dipoles where the center of the one cross lies in a direction that bisects the arms of the other cross. This configuration is known to minimize mutual coupling [5]. It is seen that the MSA concept approximates the coupling in this particular case. Of course, the calculations carried out here cannot explain the variation in mutual impedance when the relative orientation between the crosses is changed, since only rotationally symmetric patterns have been considered.

#### Helices

The phase of  $Z_{12}$  has not been used until now, but comes into play of course when the combined pattern of several antennas is studied. In this section small helices are used.

The measured pattern of a one-wavelength-long helix on a pseudo-rectangular groundplane of size  $3.0\lambda \times 0.8\lambda$  is shown in Fig. 6(a). Because of the nulls a power pattern of the form

$$P(\theta) = 1 + A \cos^N \theta + B \cos^{2N} \theta \tag{7}$$

has been assumed, rather than (2). The constants  $A, B$ , and  $N$  have been determined to make a best fit to the measured pattern, bearing in mind that an infinite groundplane (as is used in the present formulation) tends to broaden the main lobe compared to the finite groundplane used in the experiment. Therefore the fitted pattern in Fig. 6(a) has slightly shifted minima positions.

Now the pattern of a two-element array is computed, where one antenna is driven and the other resistively terminated. The relative strength of the parasitic element is  $-Z_{12}/Z$ , and the values of  $A, B$ , and  $N$  found in the preceding are used. The result for  $d = 0.568\lambda$  is shown in Fig. 6(b) and for  $d = 0.75\lambda$  in Fig. 6(c). The agreement is surprising, taking into account the complexity of the coupling; a complete numerical evaluation of the scattered field would have been very time-consuming.

### CONCLUSION

It has been shown that for minimum scattering antennas, power patterns may be predicted that minimize the mutual impedance between two identical antennas. It is unknown how many antenna types are adequately covered by the theory; most one-mode antennas should belong approximately. However, it has been shown by comparison with experiments that small helices are well described by the theory. For simple monotonic patterns it has been shown that an unavoidable couplings appear for  $d/\lambda < 0.5$ , while for  $d/\lambda > 0.5$  one may always find a pattern which essentially leads to zero coupling.

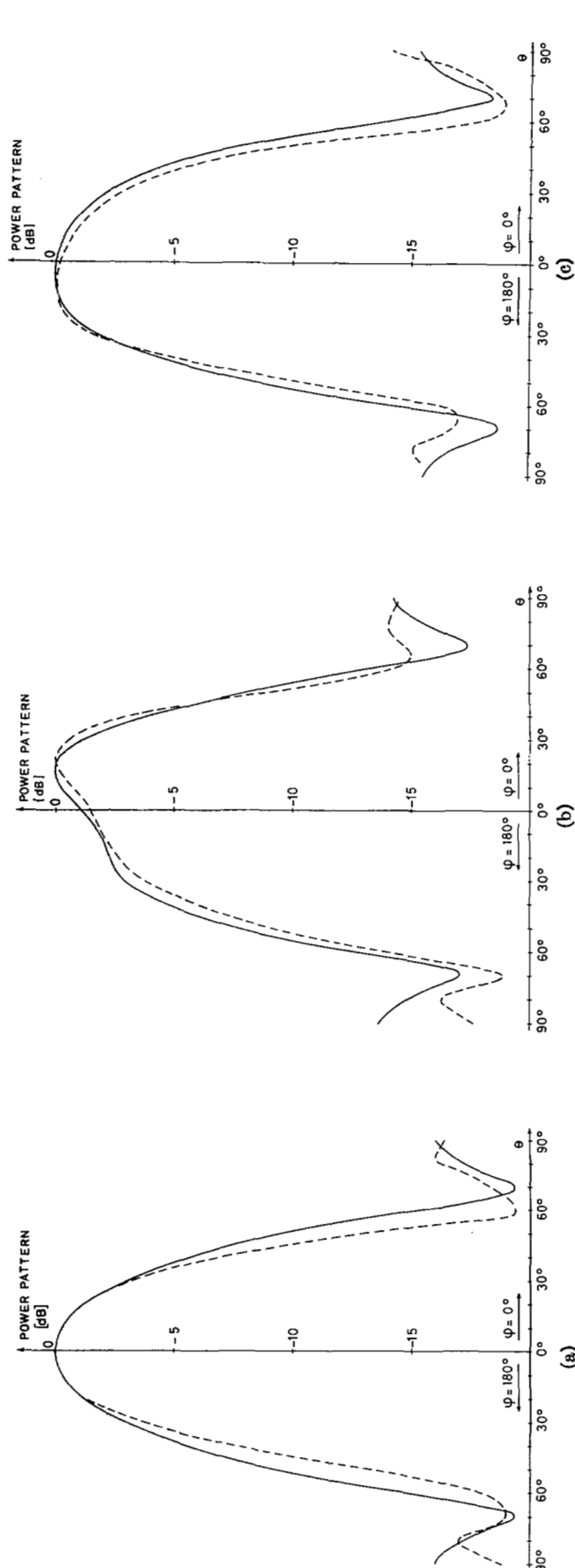


Fig. 6. (a) --- Measured pattern for one helix. --- 'fitted' pattern for one helix. (b) --- Measured pattern for two helices. --- Calculated pattern for two helices. (c) --- Calculated pattern for two helices.

## ACKNOWLEDGMENT

V. St. André, Thomson-CSF, France, is gratefully acknowledged for having supplied the measurements on small helices.

## REFERENCES

- [1] C. G. Montgomery, R. H. Dicke, and E. M. Purcell, Eds., *Principles of Microwave Circuits*. New York: Dover, 1965, pp. 317-333.
- [2] W. Wasylkiwskyj and W. K. Kahn, "Theory of mutual coupling among minimum-scattering antennas," *IEEE Trans. Antennas Propagat.*, vol. AP-18, pp. 204-216, Mar. 1970.
- [3] —, "Scattering properties and mutual coupling of antennas with prescribed radiation pattern," *IEEE Trans. Antennas Propagat.*, vol. AP-18, pp. 741-752, Nov. 1970.
- [4] J. Bach Andersen, H. A. Lessow, and H. Schjær-Jacobsen, "Coupling in multi-beam reflector antennas," Laboratory of Electromagnetic Theory, Technical University of Denmark, Lyngby, Tech. Rep. R 119, Aug. 1973.
- [5] J. Bach Andersen, H. Schjær-Jacobsen, and H. A. Lessow, "Coupling between crossed-dipole feeds," *IEEE Trans. Antennas Propagat.*, vol. AP-22, pp. 641-646, Sept. 1974.

### Experimental VSWR's and Radiation Patterns of an Axial Rectangular Slot on Conducting Cylinders of Varying Curvature

S. J. TETENBAUM

**Abstract**—*X* band measurements of the VSWR's and radiation patterns of an axial rectangular slot on six conducting cylinders of different curvature are reported. The cylinders had  $k_0a$  ( $k_0$  is the free-space wavenumber and  $a$  is the cylinder radius) varying from  $\infty$  to 1.5. Measurements were performed both with the slot bare and with the slot covered by space cloth. For  $k_0a$  as low as 3, the effect of curvature was relatively small. Below  $k_0a \approx 3$ , changes in the VSWR and radiation pattern were more pronounced, the pattern being relatively more sensitive to changes in  $k_0a$  than the VSWR.

## INTRODUCTION

A number of investigators have considered whether a bare or plasma-covered axial rectangular slot on a conducting cylinder can be treated as if the cylindrical surface is replaced by a flat ground plane. Fante [1] compared the calculated admittance of the slot for different values of  $k_0a$ . He found that for a number of representative plasma-covered slots, the ground plane ( $k_0a = \infty$ ) value of the admittance was usually within 20 percent of the cylindrical value, even for  $k_0a$  as small as 1.5. Croswell *et al.* [2] calculated the admittance of slots of two different dimensions over a wide range of  $k_0a$  and underdense lossless homogeneous plasmas. They found that for  $k_0a$  down to about 2, the change in slot admittance from that for a plane was less than 20 percent. Golden and Stewart [3] compared the computed admittance of a slot on a ground plane with measured *X* band slot admittances on both a plane and a cylindrical ( $k_0a = 9.5$ ) surface. The comparison was made for a bare slot and one covered with two different space cloth simulated plasmas. Good agreement was found. Karas and Antonucci [4] measured the *J* band admittance of a slot covered by a simulated underdense lossless homogeneous plasma, for five values of  $k_0a$  ranging from 8.6 to 2.0. They utilized two contiguous real dielectrics to simulate the plasma/free space interaction. For the case of no plasma, they found that the slot admittance decreased by about 30 percent in going from  $k_0a = 8.6$  to  $k_0a = 2.0$ , the theoretical admittance for  $k_0a = \infty$  falling between the experimental admittances for the largest and smallest  $k_0a$ . For the case of the simulated plasma, the change in admittance was generally smaller.